Journal of Computational Mathematics, Vol. 25, No. 3, 2007, 350–367.

THE USE OF PLANE WAVES TO APPROXIMATE WAVE PROPAGATION IN ANISOTROPIC MEDIA*

Tomi Huttunen
(*Department of Physics, University of Kuopio, P.O. Box 1627, FIN-70211 Kuopio, Finland
Email: tomi.huttunen@uku.fi*)

Peter Monk
(*Department of Mathematical Sciences, University of Delaware, Newark, DE 19716, USA
Email: monk@math.udel.edu*)

Abstract

In this paper we extend the standard Ultra Weak Variational Formulation (UWVF) of Maxwell's equations in an isotropic medium to the case of an anisotropic medium. We verify that the underlying theoretical framework carries over to anisotropic media (however error estimates are not yet available) and completely describe the new scheme. We then consider TM mode scattering, show how this results in a Helmholtz equation in two dimensions with an anisotropic coefficient and demonstrate how to formulate the UWVF for it. In one special case, convergence can be proved. We then show some numerical results that suggest that the UWVF can successfully simulate wave propagation in anisotropic media.

Mathematics subject classification: 65N30, 65N12
Key words: Ultra weak, Maxwell, Plane wave, Anisotropic medium.

1. Introduction

Electromagnetic wave propagation in anisotropic media arises in several applications including ground penetrating radar [3], microwave interaction with wood [13] and biological materials [20]. This paper is devoted to developing a method for approximating the electromagnetic field propagating in anisotropic media, with particular attention to microwave interactions with anisotropic (e.g. wooden) scatterers. This implies that the wavelength of the radiation is neither very large nor very small compared to features of scatterers located in the medium.

We shall develop a Discontinuous Galerkin (DG) method for the anisotropic Maxwell system with the novelty that local solutions of the anisotropic Maxwell system on each element are used as basis functions. This requires us to impose the restriction that the matrix electromagnetic parameters ϵ (permittivity) and μ (permeability) must be piecewise constant on each element in the mesh. More precisely, the method we shall develop is an extension of the Ultra Weak Variational Formulation (UWVF) of Cessenat and Després [4–6] to anisotropic media. The basic UWVF has proved to be a convenient method for approximating electromagnetic scattering in isotropic media. For example, in [17] we detail the connection of the UWVF to standard DG methods, give several extensions to the basic UWVF and provide validation results using standard electromagnetic scattering benchmark problems.

It is, of course, possible to handle anisotropic media in the classical finite element method for Maxwell's equations based on Nédélec's [26] edge elements. We have found the UWVF to

* Received November 6, 2006; Final revised February 1, 2007.

be competitive with the edge finite element method, and in [17] we show that the UWVF can be more memory efficient then edge elements and is also easily parallelized for electromagnetic applications. This motivates our extension of the UWVF to anisotropic media.

The UWVF is by no means the only technique that can be used to approximated wave propagation by using local solutions of the Maxwell system as basis functions. The UWVF resembles the basic Trefftz type finite element technique that has been applied to Maxwell's equations in [27, 28] although the variational statement is different. At least for the Helmholtz equation, other methods include least squares techniques [21, 25, 30] and enriched finite element methods [31, 32]. In a different direction, the Partition of Unity Finite Element Method (PUFEM) constructs a conforming approximation space as a product of partition of unity functions (usually finite element hat functions) and plane waves [1, 22, 23]. As yet there is probably not enough experience with the various methods to declare one preferable to another (for interesting comparison results for the Helmholtz equation in 2D see [12, 14]).

The plan of this paper is as follows. In the remainder of the introduction we shall describe in more detail the problem we shall study. Then in Section 2 we show that the fundamental mathematical result behind the UWVF for Maxwell's equations still holds for anisotropic media. This implies that the basic UWVF can be extended to anisotropic media, and we give details. In Section 3 we examine the choice of basis functions. As usual we employ a basis of plane waves on each element [4]. Plane wave propagation in anisotropic media is a classical topic in textbooks on electromagnetism (see e.g. [7, 19]). We shall summarize some of the relevant results, derive some consequences for the UWVF and then show how to use the plane waves to discretize the anisotropic UWVF. Almost all theoretical questions related to the 3D UWVF approach to anisotropic media are still open: in particular, the relevant approximation properties of sums of anisotropic plane waves are not known.

In Section 4 we discuss the case of electromagnetic wave propagation in an orthotropic medium. This reduces to solving the Helmholtz equation in two dimensions with an anisotropic "diffusion" coefficient. This problem can also be approximated by an extension of the UWVF in [4] to orthotropic media (or by a restriction of the above mentioned 3D UWVF to the orthotropic case). In contrast to the 3D case, the known convergence theory for the 2D Helmholtz UWVF can be extended to the anisotropic case in one case. We summarize the main steps and results.

In Section 5 we present some preliminary numerical results for an orthotropic medium. These results show that the UWVF is a promising method for dealing with anisotropic media. One interesting result is that since we can view the Perfectly Matched Layer (PML) [2, 24] as a special (non-physical) anisotropic medium, it can be implemented in a general anisotropic code without further modification. Our results show that this method of implementing the PML works as well as our previous implementation based on special plane waves [16, 17].

The model problem we shall investigate is to approximate the electric and magnetic fields $\boldsymbol{E}$ and $\boldsymbol{H}$ (appropriately scaled [24]) that satisfy the Maxwell system

$$\left.\begin{array}{r} -ik\epsilon_r\boldsymbol{E} - \nabla\times\boldsymbol{H} = 0 \\ -ik\mu_r\boldsymbol{H} + \nabla\times\boldsymbol{E} = 0 \end{array}\right\} \text{ in } \Omega, \tag{1.1}$$

where Ω is a bounded polyhedral domain. Here k is the wave-number of the radiation that is related to the temporal frequency $\omega > 0$, the permittivity of free space ϵ_0 and the permeability of free space μ_0 by $k = \omega\sqrt{\epsilon_0\mu_0}$. The relative permittivity ϵ_r is assumed to be a complex valued matrix function of position $\boldsymbol{x}$ in Ω. In particular

$$\epsilon_r(x) = \left(\frac{1}{\epsilon_0}\epsilon(\boldsymbol{x}) + \frac{i}{\omega\epsilon_0}\sigma(\boldsymbol{x})\right),$$

where $\sigma(x)$ is the conductivity and $\epsilon(\boldsymbol{x})$ is the permittivity of the material at $\boldsymbol{x}$. Both $\epsilon(\boldsymbol{x})$ and $\sigma(\boldsymbol{x})$ can be real symmetric matrices and physically we can assume that ϵ is strictly positive definite and σ is positive semi-definite. In an isotropic medium both ϵ and σ are multiples of the identity matrix. In the same way the relative permeability $\mu_r(x) = \mu_0^{-1}\mu(x)$ and is assumed to be a real strictly positive definite matrix function of position (ruling out ferromagnetic media - although we shall briefly comment on extending to this case later). Due to limitations in the UWVF we also need to assume that ϵ_r and μ_r are piecewise constant matrix functions of position.

Besides the Maxwell system (1.1) we also need a boundary condition on $\Gamma = \partial\Omega$. Denoting by $\boldsymbol{n}$ the unit outward normal to Ω on the boundary Γ, the boundary condition we shall use is written as

$$\begin{aligned} &-\boldsymbol{E}\times\boldsymbol{n} + \gamma(\boldsymbol{H}\times\boldsymbol{n})\times\boldsymbol{n} \\ &= Q(\boldsymbol{E}\times\boldsymbol{n} + \gamma(\boldsymbol{H}\times\boldsymbol{n})\times\boldsymbol{n}) + \boldsymbol{g} \quad \text{on } \Gamma = \partial\Omega, \end{aligned} \tag{1.2}$$

where Q, $|Q| \le 1$, is a real valued scalar function of position on Γ, $\gamma > 0$ is a strictly positive real valued function of position and $\boldsymbol{g} \in L_t^2(\Gamma)$ is a given tangential field ($L_t^2(\Gamma)$ is defined, as usual, to be the space of vector functions in $\left(L^2(\Gamma)\right)^3$ with zero normal component almost everywhere on Γ). The above boundary condition can be rewritten in the more standard form

$$-\boldsymbol{E}\times\boldsymbol{n} + Z(\boldsymbol{H}\times\boldsymbol{n})\times\boldsymbol{n} = \boldsymbol{f},$$

where $\boldsymbol{f} = (1+Q)^{-1}\boldsymbol{g}$ and the surface impedance Z is given by

$$Z = \left(\frac{1-Q}{1+Q}\right)\gamma, \quad Q \neq -1,$$

showing that the boundary condition (1.2) is just a convenient form of the standard impedance boundary condition that includes both perfectly conducting and magnetic wall boundary conditions.

2. Derivation of the UWVF for Anisotropic Media

Our first goal is to derive the continuous UWVF applied to Maxwell's equations in an anisotropic medium. The crucial point is that a suitable "Isometry Lemma" holds. We start by covering Ω by a mesh of tetrahedra denoted $\mathcal{T}_h$. The elements in $\mathcal{T}_h$ are assumed to be regular and have a maximum radius h (i.e. the radius of the circumscribed sphere for each element in $\mathcal{T}_h$ is less than h). We also assume that the mesh is such that ϵ_r and μ_r are constant on each element $K \in \mathcal{T}_h$. In our numerical examples the mesh is provided by a finite element mesh generator, so it is, in fact, a conforming tetrahedral grid in 3D and a triangular grid in 2D.

Let K denote an element in the mesh with boundary ∂K and outward normal $\boldsymbol{n}^K$. Let $\boldsymbol{\psi}$ and $\boldsymbol{\xi}$ denote smooth vector functions of position in K and let γ denote a strictly positive real valued function on ∂K (we shall make precise our choice shortly, but on Γ the choice of γ is determined by the boundary condition (1.2)). Then direct calculation shows that

$$\begin{aligned}
&\int\limits_{\partial K} \frac{1}{\gamma}(\boldsymbol{E}\times\boldsymbol{n}^K+\gamma(\boldsymbol{H}\times\boldsymbol{n}^K)\times\boldsymbol{n}^K)\cdot\overline{(\boldsymbol{\xi}\times\boldsymbol{n}^K+\gamma(\boldsymbol{\psi}\times\boldsymbol{n}^K)\times\boldsymbol{n}^K)}\,dA\\
=&\int\limits_{\partial K} \frac{1}{\gamma}(-\boldsymbol{E}\times\boldsymbol{n}^K+\gamma(\boldsymbol{H}\times\boldsymbol{n}^K)\times\boldsymbol{n}^K)\cdot\overline{(-\boldsymbol{\xi}\times\boldsymbol{n}^K+\gamma(\boldsymbol{\psi}\times\boldsymbol{n}^K)\times\boldsymbol{n}^K)}\,dA\\
&-2\int\limits_{\partial K}(\boldsymbol{E}\times\boldsymbol{n}^K\cdot\bar{\boldsymbol{\psi}}+\boldsymbol{H}\cdot\bar{\boldsymbol{\xi}}\times\boldsymbol{n}^K)\,dA,
\end{aligned}$$

where the over-bar denotes complex conjugation, and we have used the fact that $(\boldsymbol{H}\times\boldsymbol{n}^K)\times\boldsymbol{n}^K=-\boldsymbol{H}_T$ where $\boldsymbol{H}_T$ is the tangential component of $\boldsymbol{H}$ on ∂K (and similarly for $\boldsymbol{\psi}$). Using the standard integral identity that for any sufficiently smooth vector functions $\boldsymbol{a}$ and $\boldsymbol{b}$ (in particular if the two functions are square integrable and have a square integrable curl)

$$\int_K \nabla\times\boldsymbol{a}\cdot\boldsymbol{b}\,dV=\int_{\partial K}\boldsymbol{n}^K\times\boldsymbol{a}\cdot\boldsymbol{b}\,dA+\int_K\boldsymbol{a}\cdot\nabla\times\boldsymbol{b}\,dV$$

and then using the Maxwell system (1.1) we obtain

$$\begin{aligned}
&\int\limits_{\partial K}\boldsymbol{E}\times\boldsymbol{n}^K\cdot\bar{\boldsymbol{\psi}}+\boldsymbol{H}\cdot\bar{\boldsymbol{\xi}}\times\boldsymbol{n}^K\,dA\\
=&\int\limits_K \boldsymbol{E}\cdot\nabla\times\bar{\boldsymbol{\psi}}-\nabla\times\boldsymbol{E}\cdot\bar{\boldsymbol{\psi}}+\nabla\times\boldsymbol{H}\cdot\bar{\boldsymbol{\xi}}-\boldsymbol{H}\cdot\nabla\times\bar{\boldsymbol{\xi}}\,dV\\
=&\int\limits_K \boldsymbol{E}\cdot(\nabla\times\bar{\boldsymbol{\psi}}-ik\epsilon_r\bar{\boldsymbol{\xi}})-\boldsymbol{H}\cdot(\nabla\times\bar{\boldsymbol{\xi}}+ik\mu_r\bar{\boldsymbol{\psi}})\,dV.
\end{aligned}$$

Thus if we choose $\boldsymbol{\xi}$ and $\boldsymbol{\psi}$ to be smooth solutions of the adjoint Maxwell system

$$\left.\begin{aligned}-ik\bar{\epsilon}_r\boldsymbol{\xi}-\nabla\times\boldsymbol{\psi}=0\\ -ik\bar{\mu}_r\boldsymbol{\psi}+\nabla\times\boldsymbol{\xi}=0\end{aligned}\right\}\text{ in } K, \tag{2.1}$$

we have verified the conclusion of the following "Isometry Lemma" (c.f. Théorèm 13 of [4]).

Lemma 2.1 (Isometry Lemma) *Suppose* $(\boldsymbol{\xi},\boldsymbol{\psi})$ *is a smooth solution of* (2.1) *and that* $(\boldsymbol{E},\boldsymbol{H})$ *is a square integrable solution of (1.1) with square integrable curl and such that* $\boldsymbol{E}\times\boldsymbol{n}^K+\gamma(\boldsymbol{H}\times\boldsymbol{n}^K)\times\boldsymbol{n}^K)\in L^2_t(\partial K)$. *Then the following identity holds*

$$\begin{aligned}
&\int\limits_{\partial K} \frac{1}{\gamma}(\boldsymbol{E}\times\boldsymbol{n}^K+\gamma(\boldsymbol{H}\times\boldsymbol{n}^K)\times\boldsymbol{n}^K)\cdot\overline{(\boldsymbol{\xi}\times\boldsymbol{n}^K+\gamma(\boldsymbol{\psi}\times\boldsymbol{n}^K)\times\boldsymbol{n}^K)}\,dA\\
=&\int\limits_{\partial K} \frac{1}{\gamma}(-\boldsymbol{E}\times\boldsymbol{n}^K+\gamma(\boldsymbol{H}\times\boldsymbol{n}^K)\times\boldsymbol{n}^K)\cdot\overline{(-\boldsymbol{\xi}\times\boldsymbol{n}^K+\gamma(\boldsymbol{\psi}\times\boldsymbol{n}^K)\times\boldsymbol{n}^K)}\,dA.
\end{aligned}$$

The UWVF can now be constructed in the usual way with the only change being the appropriate modified adjoint problem. More precisely, for each element K, let

$$\mathcal{X}^K=\boldsymbol{E}\times\boldsymbol{n}^K+\gamma(\boldsymbol{H}\times\boldsymbol{n}^K)\times\boldsymbol{n}^K$$

and let $\mathcal{Y}^K \in L^2_t(\partial K)$ denote any vector test function. Then let $(\boldsymbol{\xi}, \boldsymbol{\psi})$ solve the adjoint Maxwell system (2.1) together with the boundary condition

$$\boldsymbol{\xi} \times \boldsymbol{n}^K + \gamma(\boldsymbol{\psi} \times \boldsymbol{n}^K) \times \boldsymbol{n}^K = \mathcal{Y}^K \quad \text{on} \quad \partial K.$$

We can then define $F^K : L^2_t(\partial K) \to L^2_t(\partial K)$ by

$$F^K(\mathcal{Y}^K) = -\boldsymbol{\xi} \times \boldsymbol{n}^K + \gamma(\boldsymbol{\psi} \times \boldsymbol{n}^K) \times \boldsymbol{n}^K \quad \text{on} \quad \partial K.$$

Following Cessenat [4] and using the Isometry Lemma and the above definitions we have

$$\int\limits_{\partial K} \frac{1}{\gamma} \mathcal{X}^K \cdot \overline{\mathcal{Y}^K}\, dA = \int\limits_{\partial K} \frac{1}{\gamma}(-\boldsymbol{E} \times \boldsymbol{n}^K + \gamma(\boldsymbol{H} \times \boldsymbol{n}^K) \times \boldsymbol{n}^K) \cdot \overline{F^K(\mathcal{Y}^K)}\, dA. \tag{2.2}$$

Although this has been derived for smooth $\mathcal{Y}^K$, this expression is well defined for $\mathcal{Y}^K \in L^2_t(\partial K)$ provided $\mathcal{X}^K \in L^2_t(\partial K)$ and hence we may extend the conclusion of the Isometry Lemma to this case. Recalling that if K' is another element in the mesh and $K' \cap K = f$ where f is a face in the mesh then $\boldsymbol{n}^K = -\boldsymbol{n}^{K'}$ so using the continuity of tangential electric and magnetic fields across surfaces for solutions of (1.1) we have

$$-\boldsymbol{E} \times \boldsymbol{n}^K + \gamma(\boldsymbol{H} \times \boldsymbol{n}^K) \times \boldsymbol{n}^K = \boldsymbol{E} \times \boldsymbol{n}^{K'} + \gamma(\boldsymbol{H} \times \boldsymbol{n}^{K'}) \times \boldsymbol{n}^{K'} = \mathcal{X}^{K'}.$$

Similarly for a face f of K on the boundary Γ the boundary condition (1.2) gives

$$-\boldsymbol{E} \times \boldsymbol{n}^K + \gamma(\boldsymbol{H} \times \boldsymbol{n}^K) \times \boldsymbol{n}^K = Q\mathcal{X}^K + \boldsymbol{g}.$$

Thus the term $-\boldsymbol{E} \times \boldsymbol{n}^K + \gamma(\boldsymbol{H} \times \boldsymbol{n}^K) \times \boldsymbol{n}^K$ in (2.2) can be replaced using $\mathcal{X}^K$, $\mathcal{X}^{K'}$ and data as appropriate.

It remains to choose the strictly positive real scalar function γ for each face on the mesh (in fact γ could be a symmetric positive definite matrix provided we interpret $1/\gamma$ as γ^{-1} and γ maps tangential vector fields to tangential vector fields, but we currently see no advantage to this choice). On the boundary, γ is given by the boundary condition. For interior element faces the choice is somewhat arbitrary. Motivated by the standard absorbing boundary condition whenever a face is between two elements in free space we choose

$$\gamma = \sqrt{\mu_0/\epsilon_0}.$$

For faces separating two elements K and K' with different possibly anisotropic electromagnetic properties we suggest

$$\gamma = \sqrt{\frac{\|\mu_r|_K\| \|\mu_r|_{K'}\|}{\|\epsilon_r|_K\| \|\epsilon_r|_{K'}\|}},$$

where $\|\cdot\|$ denotes a convenient matrix norm (for example the natural infinity norm), although the best choice has yet to be determined.

Using (2.2) and the above observations, we that $\mathcal{X}^K \in L^2_t(\partial K)$, $K \in \mathcal{T}_h$ satisfies

$$\int\limits_{\partial K} \frac{1}{\gamma} \mathcal{X}^K \overline{\mathcal{Y}^K}\, dA - \sum_{\substack{K' \in \mathcal{T}_h \\ \partial K \cap \partial K' = f \neq \phi}} \int_f \frac{1}{\gamma} \mathcal{X}^{K'} \overline{F^K(\mathcal{Y}^K)}\, dA$$
$$- \sum_{\partial K \cap \Gamma = f \neq \phi} \int_f \frac{1}{\gamma} Q\mathcal{X}^K \overline{F^K(\mathcal{Y}^K)}\, dA = \int_{\partial K \cap \Gamma} \frac{1}{\gamma} g\overline{F^K(\mathcal{Y}^K)}\, dA, \tag{2.3}$$

for all $\mathcal{Y}^K \in L_t^2(\partial K)$ and all $K \in \mathcal{T}_h$. This provides a system of variational equations for $\mathcal{X}^K$. For an isotropic medium and the above described choice of γ, (2.3) is exactly the UWVF of [4, 6].

The UWVF system (2.3) is proved to have a unique solution in [4] this proof uses the Isometry Lemma which we have verified in this case, and hence carries over to the anisotropic UWVF. We also remark that if μ_r is not symmetric, the term $\bar{\mu}_r$ in the adjoint Maxwell system (2.1) needs to be replaced by $(\bar{\mu}_r)^T$ where the superscript T denotes transpose. Hence the UWVF could perhaps also be extended to ferromagnetic media.

3. Discrete UWVF for Anisotropic Media

To obtain a discrete UWVF we need to develop a set of solutions of the adjoint Maxwell system that is convenient for computation (in particular allowing F^K to be easily evaluated) and that can be used to approximate functions in $L_t^2(\partial K)$, for each $K \in \mathcal{T}_h$. As in the case of the standard UWVF we use the plane waves. We assume that

$$\boldsymbol{\xi}(\boldsymbol{x}) = \boldsymbol{p}\exp(iK\boldsymbol{d}\cdot\boldsymbol{x}), \quad \boldsymbol{\psi}(\boldsymbol{x}) = \boldsymbol{q}\exp(iK\boldsymbol{d}\cdot\boldsymbol{x}), \tag{3.1}$$

where $\boldsymbol{d}$, $|\boldsymbol{d}| = 1$ is a given direction vector, K is a wave-number to be determined and $\boldsymbol{p}$ and $\boldsymbol{q}$ are polarization vectors also to be determined. Since $\boldsymbol{\xi}$ and $\boldsymbol{\psi}$ are required to satisfy the adjoint Maxwell system the unknowns $\boldsymbol{p}$, $\boldsymbol{q}$ and K must satisfy

$$\left.\begin{aligned} -k\bar{\epsilon}_r\boldsymbol{p} - K\boldsymbol{d}\times\boldsymbol{q} = 0, \\ -k\bar{\mu}_r\boldsymbol{q} + K\boldsymbol{d}\times\boldsymbol{p} = 0, \end{aligned}\right\} \tag{3.2}$$

where we recall that ϵ_r and μ_r are constant matrices on K. Note that in contrast to an isotropic medium $\boldsymbol{p}$ and $\boldsymbol{q}$ are not necessarily orthogonal to the direction of propagation $\boldsymbol{d}$.

Let A and B denote 6×6 matrices given by

$$A = \left(\begin{array}{c|c} 0 & -C \\ \hline C & 0 \end{array}\right), \text{ with } C = \begin{pmatrix} 0 & -d_3 & d_2 \\ d_3 & 0 & -d_1 \\ -d_2 & d_1 & 0 \end{pmatrix}$$

and

$$B = \left(\begin{array}{c|c} \bar{\epsilon}_r & 0 \\ \hline 0 & \bar{\mu}_r \end{array}\right).$$

Then (3.2) can be written as

$$KA\boldsymbol{x} = kB\boldsymbol{x},$$

where $\boldsymbol{x} = (\boldsymbol{p}, \boldsymbol{q})^T$. This leads to solving the generalized eigenvalue problem of finding $\boldsymbol{x} \neq 0$ and λ such that

$$A\boldsymbol{x} = \lambda B\boldsymbol{x}. \tag{3.3}$$

For a given eigenvector $\boldsymbol{x}$ and non-zero eigenvalue λ we have $K = k/\lambda$ where K gives the equivalent wave number and $\boldsymbol{p}$ and $\boldsymbol{q}$ gives the polarization of the plane wave solutions in (3.1).

Note that since $C\boldsymbol{p} = \boldsymbol{d}\times\boldsymbol{p}$ we know that $C\boldsymbol{p} = 0$ if and only if $\boldsymbol{p}$ is a multiple of $\boldsymbol{d}$. Thus $\lambda = 0$ is an eigenvalue of multiplicity 2 with eigenspace spanned by $(\boldsymbol{d}, 0)^T$ and $(0, \boldsymbol{d})^T$. This leaves four non-zero eigenvalues for (3.3). However these remaining eigenvalues are paired, since if $(\lambda, \boldsymbol{p}, \boldsymbol{q})$ is an eigen-triple for (3.3) then so is $(-\lambda, -\boldsymbol{p}, \boldsymbol{q})$ because

$$A\begin{pmatrix} -\boldsymbol{p} \\ \boldsymbol{q} \end{pmatrix} = \begin{pmatrix} -C\boldsymbol{q} \\ -C\boldsymbol{p} \end{pmatrix} = \lambda \begin{pmatrix} \bar{\epsilon}_r \boldsymbol{p} \\ -\bar{\mu}_r \boldsymbol{q} \end{pmatrix} = -\lambda B \begin{pmatrix} -\boldsymbol{p} \\ \boldsymbol{q} \end{pmatrix}.$$

We choose the eigenvalues with positive real part and we assume that, as in the isotropic case, there are two independent (but now not necessarily orthogonal) polarizations for each direction of propagation.

The preceding results are perhaps more obvious if we note that, when $\lambda \neq 0$, we can eliminate either $\boldsymbol{p}$ or $\boldsymbol{q}$ in (3.2) to obtain the 3×3 eigensystems

$$C^T \bar{\mu}_r^{-1} C\boldsymbol{p} = \lambda^2 \bar{\epsilon}_r \boldsymbol{p}, \tag{3.4}$$

$$C^T \bar{\epsilon}_r^{-1} C\boldsymbol{q} = \lambda^2 \bar{\mu}_r \boldsymbol{q}, \tag{3.5}$$

where we have used the fact that $C^T = -C$. In both cases $\lambda = 0$ remains an eigenvalue with corresponding eigenvector $\boldsymbol{d}$. Once the eigenvalue λ^2 and eigenvector $\boldsymbol{p}$ (or $\boldsymbol{q}$) are determined from (3.4) or (3.5) it is easy to obtain $\boldsymbol{q}$ (or $\boldsymbol{p}$) using (3.2). We thus assume that we can compute two eigentriples $(K_1, \boldsymbol{p}^{(1)}, \boldsymbol{q}^{(1)})$ and $(K_2, \boldsymbol{p}^{(2)}, \boldsymbol{q}^{(2)})$ with $\{\boldsymbol{p}^{(1)}, \boldsymbol{p}^{(2)}\}$ forming an independent set and $K_1 \neq 0$, $K_2 \neq 0$. This is obvious if ϵ_r and μ_r are real symmetric because then (3.4) or (3.5) can be reduced to a standard eigenvalue problem for a symmetric matrix but otherwise still needs to be proved.

It remains to choose the normalization of the eigenvectors $(\boldsymbol{p}^{(j)}, \boldsymbol{q}^{(j)}), j = 1, 2$. Note we cannot choose $|\boldsymbol{p}^{(j)}| = |\boldsymbol{q}^{(j)}| = 1$. Motivated by equation (3.3) we could choose

$$(\bar{\boldsymbol{p}}^{(j)})^T Re(\epsilon_r)\boldsymbol{p}^{(j)} + (\bar{\boldsymbol{q}}^{(j)})^T Re(\mu_r)\boldsymbol{q}^{(j)} = 1.$$

An alternative would be to weight say $|\boldsymbol{p}^{(j)}| = 1$ then $|\boldsymbol{q}^{(j)}| = |\mu_r^{-1}(K/\omega)\boldsymbol{d} \times \boldsymbol{p}^{(j)}|$. The best choice of weight from the point of view of conditioning of the algorithm needs to be determined.

We now choose the plane waves

$$\left.\begin{array}{r} \boldsymbol{\xi}^{(j)}(\mathbf{x}) = \boldsymbol{p}^{(\mathbf{j})} \exp(i\mathbf{K_j}\boldsymbol{d} \cdot \boldsymbol{x}) \\ \boldsymbol{\psi}^{(j)}(\boldsymbol{x}) = \boldsymbol{q}^{(j)} \exp(iK_j \boldsymbol{d} \cdot \boldsymbol{x}) \end{array}\right\} \; j = 1, 2,$$

which gives us the two necessary plane-wave solutions for each $\boldsymbol{d}$ for use in the UWVF.

Even though $(\boldsymbol{d}, \boldsymbol{p}, \boldsymbol{q})$ are not mutually orthogonal, we do have, for $\lambda \neq 0$ in (3.3),

$$\begin{pmatrix} \boldsymbol{d} \\ 0 \end{pmatrix}^T A \begin{pmatrix} \boldsymbol{p} \\ \boldsymbol{q} \end{pmatrix} = \lambda \begin{pmatrix} \boldsymbol{d} \\ 0 \end{pmatrix}^T B \begin{pmatrix} \boldsymbol{p} \\ \boldsymbol{q} \end{pmatrix},$$

so since $\boldsymbol{d} \cdot C\boldsymbol{p} = \boldsymbol{d} \cdot \boldsymbol{d} \times \boldsymbol{p} = 0$ for any $\boldsymbol{p}$ we see that $\boldsymbol{d} \cdot \bar{\epsilon}_r \boldsymbol{p} = 0$ and similarly $\boldsymbol{d} \cdot \bar{\mu}_r \boldsymbol{q} = 0$. This is just a statement that the divergence conditions $\nabla \cdot \bar{\epsilon}_r \boldsymbol{\xi}^{(j)} = 0$ and $\nabla \cdot \overline{\mu}_r \boldsymbol{\psi}^{(j)} = 0$ hold as is to be expected for solutions of the adjoint Maxwell system.

In addition

$$\begin{pmatrix} \boldsymbol{q} \\ \boldsymbol{p} \end{pmatrix}^T A \begin{pmatrix} \boldsymbol{p} \\ \boldsymbol{q} \end{pmatrix} = -\boldsymbol{q}^T C \boldsymbol{q} + \boldsymbol{p}^T C \boldsymbol{p} = 0,$$

so $\boldsymbol{q} \cdot \bar{\epsilon}_r \boldsymbol{p} = 0$ and $\boldsymbol{p} \cdot \bar{\mu}_r \boldsymbol{q} = 0$.

As in the classical UWVF a number of directions p^K is chosen for each element K in the mesh and directions $\boldsymbol{d}_\ell^K$, $1 \leq \ell \leq p^K$ on the unit sphere are then chosen. We use the optimal spherical codes from [29]. In previous papers [17, 18] we have reported that the UWVF can suffer from matrix ill-conditioning if p^K is chosen too large. We expect the heuristics adopted, for example, in [17] will prove to be necessary for anisotropic calculations. It may also be that for anisotropic media the uniformly distributed directions are no longer optimal.

Once the directions and corresponding polarizations are determined, we then have $2p^K$ basis function pairs $(\boldsymbol{\xi}^{(j,\ell)}, \boldsymbol{\psi}^{(j,\ell)})$, $1 \le j \le 2$, $1 \le \ell \le p^K$ from which to build a discrete approximation to function in $L^2_t(\partial K)$. In particular, let

$$S_h^K = \operatorname{span}\left\{\mathcal{Y}_h^K = (\boldsymbol{\xi}^{(j,\ell)} \times \boldsymbol{n}^K + \gamma(\boldsymbol{\psi}^{(j,\ell)} \times \boldsymbol{n}^K) \times \boldsymbol{n}^K)|_{\partial K},\ 1 \le j \le 2,\ 1 \le \ell \le p^K\right\},$$

then the discrete UWVF is to seek $\mathcal{X}_h^K \in S_h^K$ such that

$$\begin{aligned}\int_{\partial K} \frac{1}{\gamma}\mathcal{X}_h^K \overline{\mathcal{Y}_h^K}\, dA - \sum_{\substack{K' \in \mathcal{T}_h \\ \partial K \cap \partial K' = f \neq \phi}} \int_f \frac{1}{\gamma}\mathcal{X}_h^{K'} \overline{F^K(\mathcal{Y}_h^K)}\, dA \\ - \sum_{\partial K \cap \Gamma = f \neq \phi} \int_f \frac{1}{\gamma} Q \mathcal{X}_h^K \overline{F^K(\mathcal{Y}_h^K)}\, dA = \int_{\partial K \cap \Gamma} \frac{1}{\gamma} g \overline{F^K(\mathcal{Y}_h^K)}\, dA, \end{aligned} \tag{3.6}$$

for all $\mathcal{Y}_h^K \in S_h^K$ and all $K \in \mathcal{T}_h$. Clearly for any $\mathcal{Y}_h^K \in S_h^K$ we can easily compute $F^K(\mathcal{Y}_h^K)$ via the plane wave expansion used to defined S_h^K.

Eq. (3.6) gives rise to a matrix problem for the expansion coefficients of $\mathcal{X}_h^K$. In [4], special basis functions for S_h^K are chosen via the complex polarization that result in an improved sparsity pattern of the matrix. Given that $(\boldsymbol{d}, \boldsymbol{p}, \boldsymbol{q})$ is not generally an orthogonal set, it is no longer readily apparent that the complex polarization approach is applicable to anisotropic media. Thus we propose the simpler choice of S_h^K above and in general the use of the UWVF to solve anisotropic propagation problems will be more expensive than the corresponding isotropic code. The matrix system resulting from (3.6) can be solved using, for example, the bi-conjugate gradient method. This simple iterative scheme is easily parallelized, a necessary step in obtaining a useful algorithm, see [17] for details.

4. The Two Dimensional Case

We now present a simplified two dimensional problem. This problem will be used to test the feasibility of the anisotropic UWVF in the next section. Assuming that the fields, sources and electromagnetic parameters are independent of x_3, and that the material is orthotropic so that

$$\epsilon_r = \begin{pmatrix} \epsilon_{11} & \epsilon_{12} & 0 \\ \epsilon_{12} & \epsilon_{22} & 0 \\ 0 & 0 & \epsilon_{33} \end{pmatrix} \quad \text{and} \quad \mu_r = \begin{pmatrix} \mu_{11} & \mu_{12} & 0 \\ \mu_{12} & \mu_{22} & 0 \\ 0 & 0 & \mu_{33} \end{pmatrix},$$

the Maxwell system (1.1) can be reduced to the following Helmholtz equation in $\mathbb{R}^2$ for the third component of the magnetic field H_3:

$$\nabla \cdot M \nabla H_3 + k^2 \mu_{33} H_3 = 0 \ \text{ in } \ \Omega \subset \mathbb{R}^2, \tag{4.1}$$

where Ω is now a domain in the (x_1, x_2) plane, and

$$M = \frac{1}{\epsilon_{11}\epsilon_{22} - \epsilon_{12}^2} \begin{pmatrix} \epsilon_{11} & \epsilon_{12} \\ \epsilon_{12} & \epsilon_{22} \end{pmatrix}. \tag{4.2}$$

In this case, the magnetic field is said to have Transverse Magnetic (TM) polarization. In the case of an isotropic medium $M = \epsilon_r I$.

The two dimensional UWVF is based on a regular triangulation of Ω. We again denote the set of triangles by $\mathcal{T}_h$ (triangles having a maximum radius h). As usual for the UWVF, we assume that M is constant on each triangle K in the mesh.

On each triangle K in the mesh $\mathcal{T}_h$, we may derive an Isometry Lemma. Corresponding to the adjoint Maxwell system we need to use the anisotropic adjoint Helmholtz equation. In particular, let ξ be a smooth solution of

$$\nabla \cdot \overline{M} \nabla \xi + k^2 \overline{\mu_{33}} \xi = 0 \text{ in } \Omega \subset \mathbb{R}^2, \tag{4.3}$$

where we have used the fact that M is symmetric. Using this function and similar steps to deriving the Isometry Lemma in Section 2 we obtain

$$\begin{aligned} & \int_{\partial K} \frac{1}{\gamma} (-\boldsymbol{n}^K \cdot M \nabla H_3 + ik\gamma H_3) \overline{(-\boldsymbol{n}^K \cdot M \nabla \xi + ik\gamma \xi)}\, ds \\ = & \int_{\partial K} \frac{1}{\gamma} (\boldsymbol{n}^K \cdot M \nabla H_3 + ik\gamma H_3) \overline{(\boldsymbol{n}^K \cdot M \nabla \xi + ik\gamma \xi)}\, ds, \end{aligned} \tag{4.4}$$

where $\boldsymbol{n}^K$ denotes the unit outward normal to K.

Using the impedance boundary condition (see (1.2)) written for H_3 as

$$\boldsymbol{n} \cdot M \nabla H_3 + ik\gamma H_3 = Q(-\boldsymbol{n} \cdot M \nabla H_3 + ik\gamma H_3) + g, \tag{4.5}$$

where $\boldsymbol{n}$ is the unit outward normal to $\partial\Omega = \Gamma$, $|Q| \leq 1$ and g is given data, we can now obtain the UWVF for the two dimensional Helmholtz equation. In particular, we define, for each element in the mesh,

$$\mathcal{X}^K = -\boldsymbol{n}^K \cdot M \nabla H_3 + ik\gamma H_3 \text{ on } \partial K$$

for each $K \in \mathcal{T}_h$, and

$$\mathcal{Y}^K = -\boldsymbol{n}^K \cdot M \nabla \xi + ik\gamma \xi \text{ on } \partial K.$$

Then using the isometry result (4.4), we obtain the variational problem of determining $\mathcal{X}^K \in L^2(\partial K)$ for all $K \in \mathcal{T}_h$ such that

$$\begin{aligned} & \int_{\partial K} \frac{1}{\gamma} \mathcal{X}^k \overline{\mathcal{Y}^K}\, ds - \sum_{\substack{K' \in \mathcal{T}_h \\ K' \cap K = e \neq \phi}} \int_e \frac{1}{\gamma} \mathcal{X}^{K'} \overline{F^K(\mathcal{Y}^K)}\, ds \\ & \qquad - \sum_{\partial K \cap \Gamma = e \neq \phi} \int_e \frac{1}{\gamma} Q \mathcal{X}^K \overline{F^K(\mathcal{Y}^K)}\, ds = \int_{\partial K \cap \Gamma} \frac{1}{\gamma} g \overline{F^K(\mathcal{Y}^K)}\, ds, \end{aligned} \tag{4.6}$$

for all $\mathcal{Y}^K \in L^2(\partial K)$ and $K \in \mathcal{T}_h$. Here $F^K : L^2(\partial K) \to L^2(\partial K)$ is the operator such that if

$$\begin{aligned} -\boldsymbol{n}^K \cdot M \nabla \xi + ik\gamma \xi &= \mathcal{Y}^K \text{ on } \partial K, \\ \nabla \cdot \overline{M} \nabla \xi + k^2 \overline{\mu}_{33} \xi &= 0 \text{ in } K, \end{aligned}$$

then $F^K(\mathcal{Y}^K) = \boldsymbol{n}^K \cdot M \nabla \xi + ik\gamma \xi$ on ∂K. The theory developed in the thesis of Cessenat [4–6] is based on the Isometry Lemma and having verified the lemma for orthotropic media the theory shows that the above problem has a unique solution.

As in the case of the UWVF for the Maxwell system, problem (4.6) can be discretized by using a basis of plane waves solutions of the anisotropic adjoint Helmholtz equation (4.3) in each element. The first method is obtained by proceeding as in the 3D case. So we seek plane wave solutions of (4.3) and thus assume

$$\xi = \exp(iK\boldsymbol{x}\cdot\boldsymbol{d})$$

for some direction vector $\boldsymbol{d}\in\mathbb{R}^2$, with $\|\boldsymbol{d}\| = 1$. Substitution into (4.3) gives

$$K^2\boldsymbol{d}^T\overline{M}\boldsymbol{d} = k^2\overline{\mu}_{33} \text{ and so } K = k\left(\frac{\overline{\mu}_{33}}{\boldsymbol{d}^T\overline{M}\boldsymbol{d}}\right)^{\frac{1}{2}}.$$

This gives an easy way to compute plane wave solutions of the adjoint problem and hence discrete (4.6). We use p^K direction vectors $\boldsymbol{d}_\ell^K$, $1\le\ell\le p^K$ per element, with the directions equally spaced on the unit circle.

Let

$$S_h^K = \left\{(-\boldsymbol{n}^K\cdot M\nabla\xi_h + ik\gamma\xi_h)|_{\partial K} \mid \xi_h\in \text{ span}\left\{\exp(iK\boldsymbol{x}\cdot\boldsymbol{d}_\ell^K),\ 1\le\ell\le p^K\right\}\right\}.$$

The discrete problem is then to find $\mathcal{X}_h^K\in S_h^K$ for each $K\in\mathcal{T}_h$ such that (4.6) is satisfied with $\mathcal{X}_h^K$ replacing $\mathcal{X}^K$ and for all test functions $\mathcal{Y}^K\in S_h^K$ and $K\in\mathcal{T}_h$. This problem has a unique solution using the arguments from [4].

At first sight the error estimates of [4,5] do not apply, but in the special case when M is real and symmetric positive definite we can adopt a second approach to determining the plane waves that allows the theory from [4,5] to be used. For simplicity let $\mu_{33}=1$. For real, symmetric positive definite M, there exists a unique positive definite square root $M^{1/2}$. We denote by $\tilde{K} = \{\boldsymbol{x}\mid M^{1/2}\boldsymbol{x}\in K\}$. Then it is shown in [10] that if u_0 satisfies

$$\Delta u_0 + k^2u_0 = 0 \text{ in } \tilde{K},$$

then $u(\boldsymbol{x}) = u_0(M^{-1/2}\boldsymbol{x})$ satisfies

$$\nabla\cdot M\nabla u + k^2u = 0 \text{ in } K.$$

Since the map $\boldsymbol{x}\to M^{-1/2}\boldsymbol{x}$ is linear, the domain $\tilde{K}$ is a triangle.

Because M is constant, a plane wave on $\tilde{K}$ results in an anisotropic plane wave on K. Thus we now choose a set of directions on $\tilde{K}$, say $\boldsymbol{d}_\ell^K$, $1\le\ell\le p^K$ (we use the superscript K since they will result in plane waves on K) and now use the basis functions

$$\boldsymbol{\xi}_\ell^K(\boldsymbol{x}) = \exp(ik(M^{-1/2}\boldsymbol{d}_\ell^K)\cdot\boldsymbol{x}),\quad 1\le\ell\le p^K,$$

to construct S_h^K.

The projection error estimates of [4,5] are applicable on $\tilde{K}$ and by the mapping also on K (of course with coefficients depending on M). In particular, let P_h denote the operator from $\prod_{K\in\mathcal{T}_h} L^2(\partial K)$ into $\prod_{K\in\mathcal{T}_h} S_h^K$ such that $P_h\xi|_{L^2(\partial K}$ is the best $L_2(\partial K)$ approximation of $\xi|_{\partial K}$ from S_h^K. Then if $p^K = p = 2n+1$ (i.e. the same number of plane waves are used on each element) and if $u\in C^{n+1}(\Omega)$ satisfies the anisotropic Helmholtz equation(4.1) in Ω we have

$$\left(\sum_{K\in\mathcal{T}_h}\|(I-P_h)\mathcal{X}\|^2_{L^2(\partial K)}\right)^{\frac{1}{2}} \le Ch^{n-1/2}\|u\|_{C^{n+1}(\Omega)},$$

where

$$\mathcal{X}|_{\partial K} = (-\boldsymbol{n}_k \cdot M\nabla u + ik\gamma u)|_{\partial K}.$$

Using this estimate and assuming that $|Q| \leq \delta < 1$, for some constant δ, the arguments of Cessenat and Després now show that if $\mathcal{X}_h \in \prod_{K\in\mathcal{T}_h} L^2(\partial K)$ is such that $\mathcal{X}_h|_{\partial K} = \mathcal{X}_h^K$ (i.e. the solution of the discrete UWVF equations) then for $n \geq 1$

$$\|\mathcal{X} - \mathcal{X}_h\|_{L^2(\Gamma)} \leq Ch^{n-1/2}\|u\|_{C^{n+1}(\Omega)}.$$

This shows that the two dimensional UWVF becomes higher order as n increases even for anisotropic media. Unfortunately, even though we observe convergence of the UWVF solution throughout Ω, the convergence theory is not yet proved in this generality.

The preceding estimates assume that the same number of plane waves are used in each element. In practice this can result in poorly conditioned matrix equations for the coefficients of $\mathcal{X}_h$ unless the mesh is uniform or close to uniform. In practical computations we use a variable number of directions per element, chosen so that a local condition number is well behaved [18]. We find that this choice controls the overall condition number.

5. Numerical Results

In this section, the feasibility of the anisotropic UWVF approximation is investigated via two model problems for orthotropic media. First, we study propagation of the magnetic field emitted by an infinitely long line source. Second, we investigate the scattering of the magnetic field from a box which is infinitely long in one direction. In both cases, as we have seen in the previous section, it is possible to reduce the problem to solving a single field component in a plane. In this section we shall assume that $\mu_{3,3} = 1$ and we shall also add a source term to the Helmholtz equation since one of our test cases is to compute the field from a line source. Then the anisotropic Helmholtz equation (4.1) reads

$$\nabla \cdot M\nabla H_3 + k^2 H_3 = f, \tag{5.1}$$

where M is given by (4.2) and f is a source term. In the model problems, the wave number $k = \omega\sqrt{\epsilon_0\mu_0}$ is normalized so that $k = \omega$ by assuming that $\epsilon_0 = \mu_0 = 1$. Furthermore, we also assume that $\mu_r = 1$.

On the exterior boundary of the computational domain we use the boundary condition (4.5). In the case of a lossless isotropic medium $M = \epsilon_r I$, where $\epsilon_r \in \mathbb{R}$ and I the identity matrix. Hence, the choice $\gamma = 1$, $Q = 0$ and $g = 0$ provides a low order Enquist-Majda absorbing boundary condition. For an anisotropic medium, however, a single value of γ that would lead to an acceptable absorbing boundary condition, is not obvious. Therefore, an alternative method reducing the numerical reflection of waves from the exterior boundary is needed.

A natural choice for truncating the computational domain for a code that incorporates a general anisotropic medium is the Perfectly Matched Layer (PML) proposed by Bérenger [2]. It is well known that the decay of waves in the PML is obtained by using an increasing, anisotropic absorption coefficient in the element layer(s) surrounding the actual computational domain. In particular, the anisotropic Helmholtz equation characterizing the field in the PML can be written in the form of Eq. (5.1) when $M = \mathrm{diag}\left(\frac{D_1}{D_2}, \frac{D_1}{D_2}\right)$ and $k^2 = k_0^2 D_1 D_2$. Here, we use the complex stretched of spatial variables x'_1 and x'_2 in the Cartesian PML defined as

$$x'_1 = \begin{cases} x_1 + \dfrac{i}{k_0} \int_{x_1^0}^{x_1} \sigma_1 dx_1, & |x_1| \geq x_1^0, \\ x_1, & |x_1| < x_1^0, \end{cases} \tag{5.2}$$

$$x'_2 = \begin{cases} x_2 + \dfrac{i}{k_0} \int_{x_2^0}^{x_2} \sigma_2 dx_2, & |x_2| \geq x_2^0, \\ x_2, & |x_2| < x_2^0, \end{cases} \tag{5.3}$$

where σ_1 and σ_2 are the decay parameters (constants) in the x_1- and x_2-direction, respectively and x_j^0, $1 \leq j \leq 2$ parametrizes the start of the layer. The constants D_1 and D_2 are obtained from the stretched variables as

$$D_1 = \frac{\partial x'_1}{\partial x_1} \quad \text{and} \quad D_2 = \frac{\partial x'_2}{\partial x_2}. \tag{5.4}$$

The use of a constant PML parameter σ_j, $j = 1, 2$ requires some comment. For the Maxwell system before discretization the use of a piecewise constant decay parameter still results in a perfect matching across the boundary (see for example [8,9]) but after discretization there will be a spurious reflection across the surface where σ jumps. At least for finite difference methods, this reflection is controlled by a sufficiently fine discretization near the interface and we expect this to be the case also for the UWVF. A general (for example quadratic dependence) of the absorption parameter can be allowed in the UWVF at the expense of having to compute the inner products needed to calculate matrix entries by quadrature. This significantly increases the time needed to assemble the linear system corresponding to the UWVF. In [16,17] we have found that it is usually more efficient to use a constant absorption parameter (and perhaps a slightly wider PML layer) than a more standard profile.

The best choice of decay parameters and the thickness of the PML is always an optimization problem. However, motivated by the results of [16], we choose in this study $\sigma_j = 2.0/L_j$, $j = 1, 2$, where L_j is the thickness of the PML.

All coding for following UWVF simulation is done using Matlab. The details for assembling the UWVF matrix equations are given in [5] and [18]. In this study, the UWVF matrix equation of the form $(I - D^{-1}C)X = D^{-1}b$ is solved using Matlab's backslash function.

5.1. A point source using the PML

In the first model problem, the field H_3 is emitted by a singular source at the point $\boldsymbol{x}_0$. For Eq. (5.1) the point source can be defined by setting $f = \delta(\boldsymbol{x}_0)$, where δ is the Dirac delta function. The computational domain in a 2×2 rectangle surrounded by a 0.4 units thick PML. The source is located at the point (0.5, 0.5). In Fig. 5.2, we show a solution of the problem when $M = \text{diag}(1, 2)$ and $k = 2\pi$ (so the wavelength is unity). The UWVF simulation is computed in the mesh of Fig. 5.1 using nine angularly equidistributed plane wave basis functions in all elements of the mesh (a uniform choice of the number of directions is permissible here since the elements are only lightly refined near the source). The discrete L_2-error measured at the circle with the radius $r = 0.9$ around the origin (0,0) is 0.85 %. The anisotropy of the medium can be seen from the ellipsoidal amplitude distribution of the solution in the top panels of Fig. 5.2.

To investigate the effect of the PML on the accuracy of the point source simulation, we plot the error as a function of the angular frequency ω (this also the wave number k because of the special choice of constants) in Fig. 5.3. Results are computed in an isotropic medium

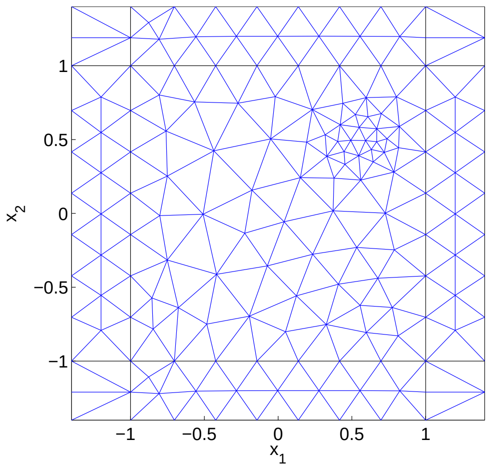

Fig. 5.1. The mesh used for the point source simulations. The mesh is refined slightly near the location of the source at (0.5, 0.5). The two outermost element layers constitute the PML.

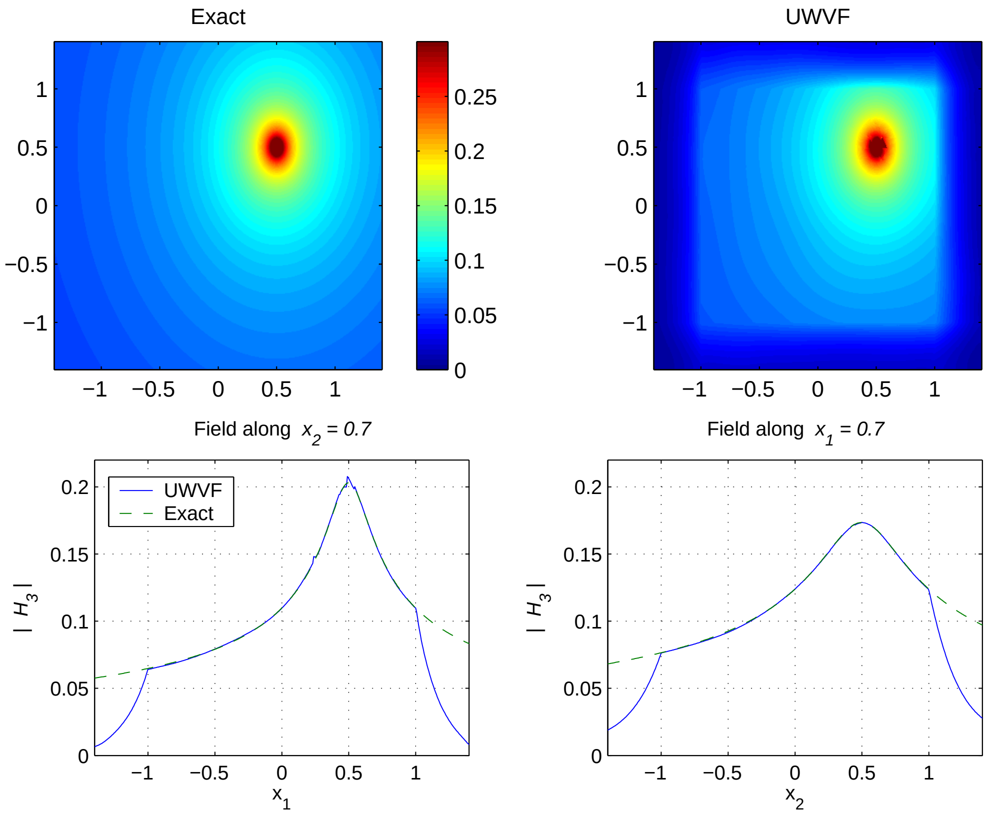

Fig. 5.2. *Top row*: The solution of the point source simulation at $k = \omega = 2\pi$. The magnitude of the exact solution is shown on the left and the UWVF approximation using the PML is on the right. A rapid decay of the amplitude of the waves can be seen in the PML ($|x_1| > 1$ and $|x_2| > 1$). *Bottom row*: The UWVF approximations for the same field $|H_3|$ along two lines crossing the computational domain and the PML.

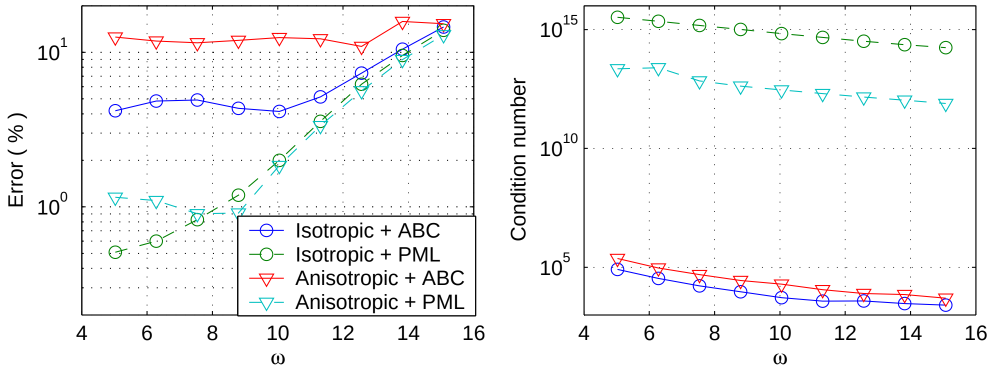

Fig. 5.3. The error and the condition number of the UWVF system matrix as a function of the angular frequency ω (or wave number k). Clearly the PML helps to improve the accuracy of the solution even in the anisotropic case, but at the cost of a higher condition number for the matrix problem.

with $\epsilon_r = 1$ and in an anisotropic medium with $M = \text{diag}(1, 2)$ by using the PML and the low order absorbing boundary condition (ABC) (4.5). In this case, we use seven plane wave basis functions in all elements of the mesh.

For the ABC, we choose $Q = 0$, $g = 0$ and

$$\gamma = \text{mean}(\hat{k}\lambda_M), \tag{5.5}$$

where $\hat{k}$ is the mean value of the directional wave numbers k_1 and k_2 and λ_M contains the eigenvalues of the matrix M. The eigenvalues λ_M are computed using Matlab's `eig`-function. The PML is implemented as an anisotropic absorbing medium as described at the start of this section. On the exterior boundary of the PML, the ABC is used with above mentioned parameters. Results show that the PML improves the accuracy but also leads to rather ill-conditioned UWVF matrices. The ill-conditioning is known to hamper methods using plane wave basis function in a strongly absorbing medium such as in the PML [15]. Plane wave basis methods can be stabilized by adjusting the number of basis functions so that the condition number remains at a low level [18]. This approach is not investigated further here.

Finally, we show the error of the anisotropic UWVF approximation as the function of the number plane wave basis functions at a fixed frequency $\omega = 2\pi$. The error shown in Figs. 5.3 and 5.4 is computed using the relative discrete L_2-norm. The error is measured at 360 points on the circle with the radius $r = 0.9$ around the origin (0,0).

5.2. Transmission

Next we consider a transmission problem modeling the scattering of electromagnetic waves by an anisotropic dielectric medium. Fig. 5.5 shows the meshed geometry used in the UWVF simulations. The computational domain consists of the 1×1 rectangular cross-section box containing an anisotropic medium which is surrounded by a circular region (with radius $r = 2$) containing a homogeneous, isotropic medium with $\epsilon_r = 1$ and $\mu_r = 1$. The permittivity matrix for the rectangle is

$$M = \begin{pmatrix} 2 & 0 \\ 0 & 8 \end{pmatrix}. \tag{5.6}$$

We compute approximations for the problem using two different incident fields consisting of respectively plane waves propagating in the direction of the positive x_1- and x_2-axis. The

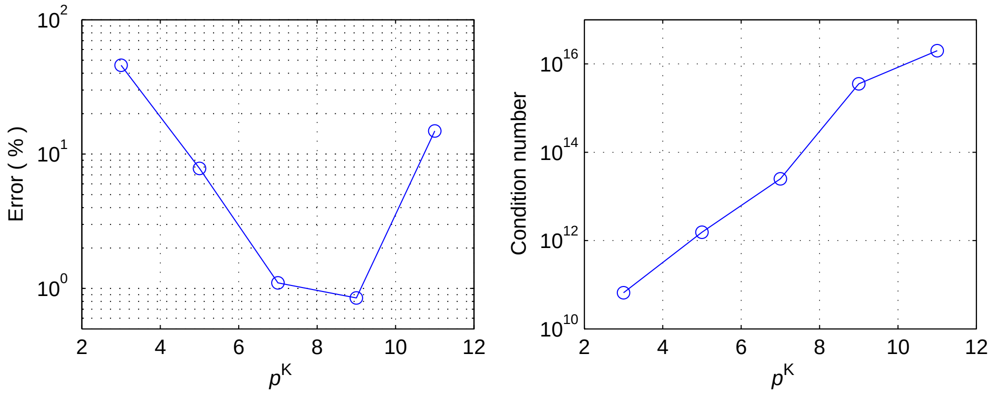

Fig. 5.4. The error and the condition number of the UWVF system matrix as a function of the number of plane wave basis functions p^K. Results are computed using the point source in an anisotropic medium with $M = \mathrm{diag}(1, 2)$ at $\omega = 2\pi$. The computational domain is truncated using the PML which leads to rather ill-conditioned UWVF matrices. Provided the condition number is not too large, increasing p^K results in a rapid improvement of the error.

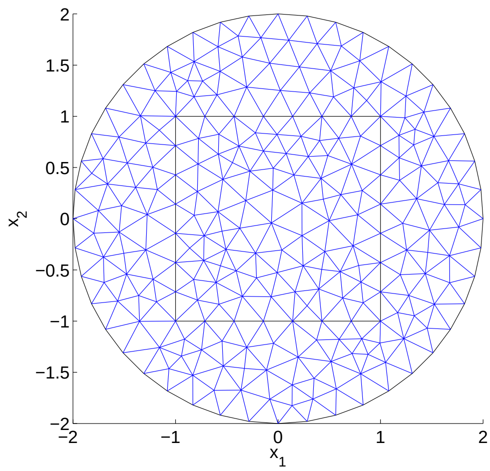

Fig. 5.5. The mesh used for the UWVF transmission simulations.

UWVF approximation and a reference finite element (FE) approximation at the angular frequency $\omega = 2\pi$ are shown in Fig. 5.6. The FE solutions are computed using a commercial finite element package (the Electromagnetic module of Comsol Multiphysics 3.2) [11]. For the FE approximation, the triangular mesh is generated so that approximately ten elements are used for the shortest wavelength of the problem (which is $\lambda_{\min} = 1/\sqrt{8}$ in the x_1-direction within the box). The FE basis is constructed from quadratic Lagrange polynomials. The UWVF approximations are computed in the mesh of Fig. 5.5. The UWVF basis for each element consists of nine angularly equispaced plane waves.

On the exterior boundary, the boundary condition (4.5) is used so that $Q = 0$, $\gamma = k$ and

$$g = \boldsymbol{n} \cdot (\nabla H_3^{\mathrm{in}}) - ikH_3^{\mathrm{in}}, \tag{5.7}$$

where $H_3^{\mathrm{in}} = \exp(ik\boldsymbol{d}\cdot\boldsymbol{x})$ with $|\boldsymbol{d}| = 1$ is the incident plane wave propagating in the direction $\boldsymbol{d}$. Note that this choice corresponds to the lowest order Enquist-Majda condition for the scattered

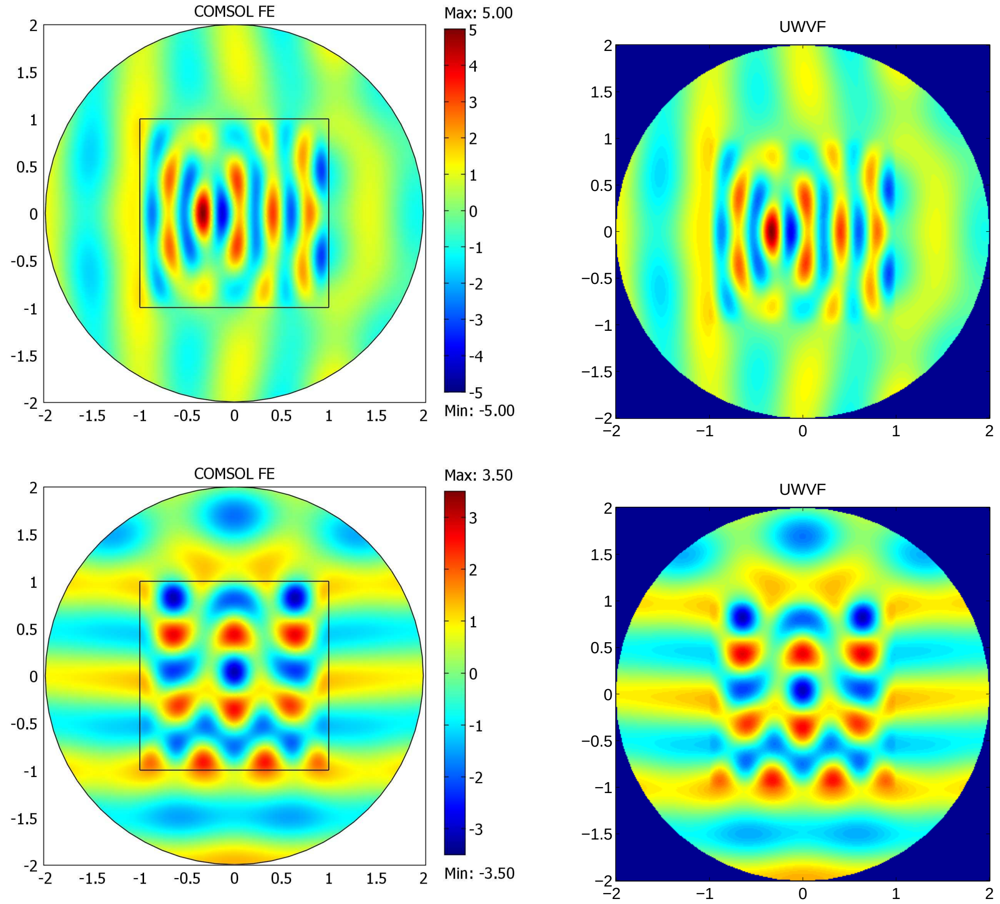

Fig. 5.6. Simulated real parts of H_3 for the anisotropic transmission problem. The first column shows the finite element approximations for the incident plane wave propagating in the positive x_1- and x_2-directions. The second column shows the corresponding UWVF approximations.

part of the magnetic field. While the use of the PML would make the model physically more realistic, the low order absorbing boundary condition is used since this condition is readily available in Comsol Multiphysics 3.2. The use of exactly same exterior boundary condition makes possible a fair comparison of the FE and UWVF methods.

A comparison of the UWVF and FE approximation in Fig. 5.6 shows a good agreement between the two methods. Both methods can capture the anisotropic features of the solution. Namely, the difference of wave speeds in x_1- and x_2-directions is clearly seen as the object is illuminated from different incident directions.

6. Conclusion

We have introduced a technique for using plane wave basis functions to approximate electromagnetic waves in an anisotropic medium. In particular, we focused on the use of the plane wave basis with the Ultra-Weak Variational Formulation. A general theory was presented for a 3D system of time-harmonic Maxwell's equations. However, the proposed method was investigated via numerical simulations for a reduced 2D system characterized by the anisotropic

Helmholtz equation. Simulations suggest that the plane waves may provide advantages over commonly used polynomial discretizations since relatively large elements can be used by increasing the number of plane wave basis functions in the large elements. This may reduce the computational burden associated with wave simulations at high wave numbers.

The anisotropic plane wave basis also have the same well-known drawbacks as their isotropic counterparts, namely, the number of basis functions for each element must be carefully adjusted to avoid the ill-conditioning resulting matrix system. In this study, the elements size of the meshes used in the simulations was relatively uniform and only moderate variation in the material properties was used within the computational domain. This allowed the use of a constant number of basis functions in all elements. In general, however, the choice of basis must be made so that the number of basis functions varies from element to element as proposed in [18]. The ill-conditioning of the problem is more severe if the computational domain contains strongly absorbing media or the PML is used. This was also observed in the simulations of this study.

Future topics of research include the numerical testing and theoretical analysis of the extension of the anisotropic plane wave basis to the 3D system of Maxwell's equations. Also an alternative choices of propagation directions for plane wave basis needs to be investigated since the angularly equispaced directions used here may not be the optimal for anisotropic waves due to the direction dependent wave speeds. For example, one may expect that the basis directions need to be more densely clustered near the direction in which the physical waves have the shortest wavelength. Finally, the performance of the plane wave basis method needs to be compared with other existing simulation methods (such as the finite element method).

Acknowledgments. Tomi Huttunen wishes to thank the Measurement and Sensor Laboratory (University of Oulu) in Kajaani for the collaboration in the field of electromagnetism and for the financial support from their Measurepolis-program. Peter Monk gratefully acknowledges the support of the Air Force Office of Scientific Research under grant number FA9550-05-1-0127.

References

[1] I. Babuška and J. Melenk, The partition of unity method, *Int. J. Numer. Meth. Engrg.*, **40** (1997), 727-758.

[2] J. Bérenger, A perfectly matched layer for the absorption of electromagnetics waves, *J. Comput. Phys.*, **114** (1994), 185-200.

[3] J. Carcione, Ground-penetrating radar: wave theory and simulation in lossy anisotropic media, *Geophysics*, **61** (1996), 1664-1677.

[4] O. Cessenat, Application d'une nouvelle formulation variationnelle aux équations d'ondes harmoniques. Problèmes de Helmholtz 2D et de Maxwell 3D, PhD thesis, Université Paris IX Dauphine, 1996.

[5] O. Cessenat and B. Després, Application of the ultra-weak variational formulation of elliptic PDEs to the 2-dimensional Helmholtz problem, *SIAM J. Numer. Anal.*, **35** (1998), 255-299.

[6] O. Cessenat and B. Després, Using plane waves as base functions for solving time harmonic equations with the Ultra Weak Variational Formulation, *J. Comput. Acoust.*, **11** (2003), 227-238.

[7] W. Chew, Waves and Fields in Inhomogeneous Media, Van Nostrand Reinhold, New York, 1990.

[8] F. Collino and P. Monk, Optimizing the perfectly matched layer, *Comput. Method. Appl. Mech. Engrg.*, **164** (1998), 157-171.

[9] F. Collino and P. Monk, The perfectly matched layer in curvilinear coordinates, *SIAM J. Sci. Comput.*, **19** (1998), 2061-2090.

[10] D. Colton, R. Kress and P. Monk, Inverse scattering from an orthotropic medium, *J. Comput. Appl. Math.*, **81** (1997), 269-298.

[11] Comsol, Homepage of COMSOL Multiphysics software, 2006, `http://www.comsol.com`.

[12] P. Gamallo and R. Astley, A comparison of two Trefftz-type methods: The ultraweak variational formulation and the least-squares method, for solving shortwave 2-D Helmholtz problems, in press.

[13] L. Hansson, N. Lundgren, A.-L. Antti and O. Hagman, Finite element modeling (FEM) simulation of interactions between wood and microwaves, *J. Wood. Sci.*, **52** (2006), 406-410.

[14] T. Huttunen, P. Gamallo and R. Astley, Comparison of two wave element methods for the Helmholtz problem, submitted.

[15] T. Huttunen, J. Kaipio and P. Monk, Parallelized UWVF method for 3D Helmholtz problems, 4th ECCOMAS, Jyvskyl, Finland, July 2004.

[16] T. Huttunen, J. Kaipio and P. Monk, The perfectly matched layer for the ultra weak variational formulation of the 3D Helmholtz equation, *Int. J. Numer. Meth. Engrg.*, **61** (2004), 1072-1092.

[17] T. Huttunen, M. Malinen and P. Monk, Solving Maxwell's equations using the Ultra Weak Variational Formulation, *J. Comput. Phys.*, 2006, to appear.

[18] T. Huttunen, P. Monk and J. Kaipio, Computational aspects of the Ultra Weak Variational Formulation, *J. Comput. Phys.*, **182** (2002), 27-46.

[19] A. Ishimaru, Electromagnetic Wave Propagation, Radiation, and Scattering, Prentice-Hall, Englewood Cliffs, 1991.

[20] A. Kaestner, Non-invasive multidimensional imaging applied on biological substances, PhD thesis, Chalmers University of Technlogy, Göteborg, Sweden, 2002.

[21] B. Lee, T. Manteuffel, S. McCormick and J. Ruge, First-order system least-squares for the Helmholtz equation, *SIAM J. Sci. Comput.*, **21** (2000), 1927-1949.

[22] J. Melenk, On generalized finite element methods, PhD thesis, University of Maryland, College Park, MD, 1995.

[23] J. Melenk and I. Babuška, The partition of unity finite element method: Basic theory and applications, *Comput. Method. Appl. Mech. Engrg.*, **139** (1996), 289-314.

[24] P. Monk, Finite Element Methods for Maxwell's Equations, Oxford University Press, Oxford, 2003.

[25] P. Monk and D. Wang, A least squares method for the Helmholtz equation, *Comput. Method. Appl. Mech. Engrg.*, **175** (1999), 121-136.

[26] J. Nédélec, Mixed finite elements in $\mathbb{R}^3$, *Numer. Math.*, **35** (1980), 315-341.

[27] V. Nikol'skiy and T. Lavrova, The method of minimum autonomous blocks and its application to wavequide diffraction problems, *Radio Engrg. Electron. Phys.*, **23** (1978), 1-10.

[28] Y. Shlepnev, Trefftz finite elements for electromagnetics, *IEEE T. Microwav Theory Techn.*, **50** (2002), 1328-1339.

[29] N. Sloane, Tables of spherical codes, with collaboration of R.H. Hardin, W.D. Smith and others, published electronically at `http://www.research.att.com/~njas/packings`, 2000.

[30] M. Stojek, Least-squares Trefftz-type elements for the Helmholtz equation, *Int. J. Numer. Meth. Engrg.*, **41** (1998), 831-849.

[31] R. Tezaur and C. Farhat, Three-dimensional discontinuous Galerkin elements with plane waves and Lagrange multipliers for the solution of mid-frequency Helmholtz problems, *Int. J. Numer. Meth. Engrg.*, **66** (2006), 796-815.

[32] L. Zhang, R. Tezaur and C. Farhat, The discontinuous enrichment method for elastic wave propagati on in the medium-frequency regime, *Int. J. Numer. Meth. Engrg.*, **66** (2006), 2086-2114.